Design and Implementation of Filters Using Transfer Functions in the Z Domain

Da-Chiang Chang and Ching-Wen Hsue, *Senior Member, IEEE*

***Abstract*—In this paper, a novel approach composed of digital signal-processing techniques and optimization algorithms is developed to design and implement filters at microwave frequencies. The design phase begins with the adoption of digital filter prototypes and the implementation phase is facilitated by using both parametric modeling techniques and optimization algorithms. All the zeros of digital filter prototypes are removed first; the remaining part of the prototypes is then transformed to an autoregressive (AR) process by parametric modeling techniques. The values of characteristic impedances of transmission lines synthesizing the filters are adjusted according to the AR process by optimization algorithms. Both low-pass and bandpass filters are designed and then implemented in the form of a microstrip line, and their frequency responses are measured to validate the novel approach.**

***Index Terms*—Microwave filter, transmission line, Z domain.**

I. Introduction

MICROWAVE filters [1] with their various responses can be fabricated in different forms; examples are bandpass or low-pass filters with nonuniform transmission lines [2], [3] and bandpass or bandstop filters with coupled lines [4], [5].

Among conventional procedures for designing microwave filters, either the image-parameter method or the insertion-loss method provide the configurations of lumped-element circuits. Once the values of lumped elements are obtained, Richard's transformation [6] is generally used to convert lumped filter elements to stubs of the same electrical length. In addition, Kuroda's identities [7], [8] can be used to separate the stubs with transmission-line sections of the same electrical length as that of the stubs. In recent years, filter design has been studied in the Z domain [9], [10] by replacing the phasor $e^{-j\theta}$ with the delay operator, and several effective interesting methods have been exploited. Actually, when stubs and transmission-line sections are manufactured with the same electrical length and are cascaded orderly, parameters describing the characteristics of the network can also be represented as functions of the delay operator. Therefore, abundant assortment of well-developed discrete-domain techniques can be applied to the studies of such networks. However, few are found in the literature.

In this paper, we first transform the chain scattering parameters of equal-electrical-length stubs and transmission-line sections to functions in the Z domain [11]. Transfer functions of the networks composed of stubs and transmission-line sections can be obtained by multiplying the chain scattering matrices of the components. Each stub contributes a zero at $z = 1$ (dc) if it is short circuited or at $z = -1$ (the unity frequency) if it is open circuited. The zeros produce steep attenuation around dc or around the unity frequency, making the networks with stubs suitable for filtering applications. For a prescribed transfer function in the Z domain, we then employ an approach comprising discrete signal processing (DSP) techniques and optimization algorithms to design and implement filters at microwave frequencies. We begin the design phase with the adoption of a digital filter prototype, which satisfies the defined specifications. We then choose a configuration for the network that is proper for the response of the filter. Both the transfer functions of the network and the digital filter prototype are divided by the terms concerning the zeros of transfer function of the network. In other words, the original zeros of the transfer function of the network are moved to the denominator of the digital filter prototype and become poles. The remaining part of the transfer function of the network is recognized to be an autoregressive (AR) process [12]. We argue that if the response of the transfer function of the network in the frequency domain is similar to that of the filter prototype, the response of the AR process will also be similar to that of the *new* function computed from the digital filter prototype by including extra poles. Based on this argument, parametric modeling algorithms are then applied to transform the new function to an AR process. The implementation process is to adjust the impedances of stubs and transmission-line sections with optimization algorithms so that the difference between the coefficients of both AR processes is as small as possible. To validate the whole process, both low-pass and bandpass filters are designed and then implemented in the form of microstrip line. Responses of the filters are measured to validate the new approach.

II. Formulation of the Transfer Function in the Z Domain

The transfer function of a cascaded network can be found by multiplying the chain scattering matrices of the components composing the network. The chain scattering parameters T_{mn}, $m, n = 1, 2$ of a two-port network are defined by assuming the waves $a(1)$ and $b(1)$ at port 1 in Fig. 1 are dependent variables, and the waves $a(2)$ and $b(2)$ at port 2 are independent variables, i.e.,

$$\begin{bmatrix} a(1) \\ b(1) \end{bmatrix} = \begin{bmatrix} T_{11} & T_{12} \\ T_{21} & T_{22} \end{bmatrix} \begin{bmatrix} b(2) \\ a(2) \end{bmatrix}. \tag{1}$$

Manuscript received February 18, 2000; revised July 10, 2000. This work was supported by the National Science Council, R.O.C. under Grant NSC 89-2213-E011-044.

The authors are with the Department of Electronic Engineering, National Taiwan University of Science and Technology, Taipei, Taiwan, R.O.C.

Publisher Item Identifier S 0018-9480(01)03314-2.

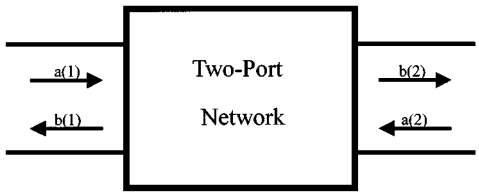

Fig. 1. Two-port network.

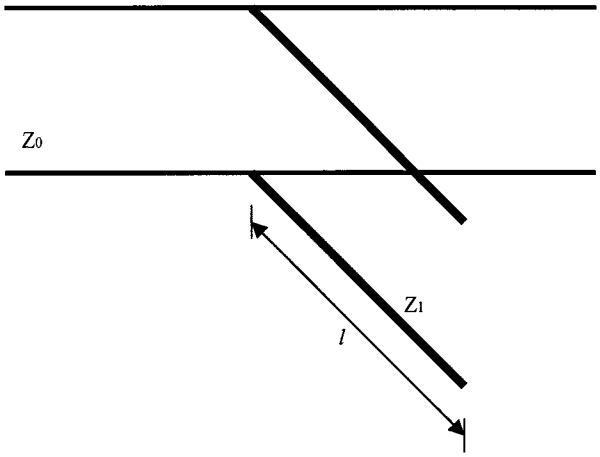

Fig. 2. Open-circuited stub.

The chain scattering matrix can be found from the scattering matrix in the following way:

$$\begin{bmatrix} T_{11} & T_{12} \\ T_{21} & T_{22} \end{bmatrix} = \begin{bmatrix} \dfrac{1}{S_{21}} & -\dfrac{S_{22}}{S_{21}} \\ \dfrac{S_{11}}{S_{21}} & S_{12} - \dfrac{S_{11}S_{22}}{S_{21}} \end{bmatrix}. \tag{2}$$

Let the length of all stubs and transmission-line sections be $l = \lambda_0/4$, where λ_0 is the wavelength of the lines at the normalizing angular frequency ω_0. In other words, the electrical length of all components is 90° at the normalizing frequency. Given the impedance of an open-circuited stub to be Z_1, shown in Fig. 2, we find that its chain scattering parameters are as follows:

$$\begin{bmatrix} T_{11} & T_{12} \\ T_{21} & T_{22} \end{bmatrix}_{\text{o.c.}} = \begin{bmatrix} 1+j\dfrac{Z_0}{2Z_1}\tan(\beta l) & j\dfrac{Z_0}{2Z_1}\tan(\beta l) \\ -j\dfrac{Z_0}{2Z_1}\tan(\beta l) & 1-j\dfrac{Z_0}{2Z_1}\tan(\beta l) \end{bmatrix} \tag{3}$$

where Z_0 is the reference characteristic impedance and β is the propagation constant. The reference planes for both ports are at the intersection of the stub and the reference transmission line.

Let ω be the angular frequency and τ be the propagation delay caused by the length l. All the terms $j\tan(\beta l) = j\tan(\omega\tau)$ can be represented in a new form by using $D^{-1} = e^{-j\omega\tau}$, which can be considered as a unit of delay, i.e.,

$$j\tan(\omega\tau) = \frac{e^{j\omega\tau} - e^{-j\omega\tau}}{e^{j\omega\tau} + e^{-j\omega\tau}} = \frac{D - D^{-1}}{D + D^{-1}}. \tag{4}$$

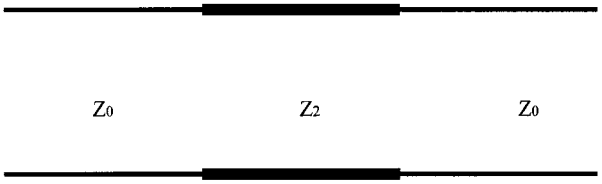

Fig. 3. Transmission-line section.

Consequently, we have

$$\begin{bmatrix} T_{11} & T_{12} \\ T_{21} & T_{22} \end{bmatrix}_{\text{o.c.}} = \frac{1}{1+D^{-2}} \begin{bmatrix} (1+c)+(1-c)D^{-2} & c-cD^{-2} \\ -c+cD^{-2} & (1-c)+(1+c)D^{-2} \end{bmatrix} \tag{5}$$

where $c = Z_0/2Z_1$.

If the stub is short circuited, its chain scattering parameters can be expressed as follows:

$$\begin{bmatrix} T_{11} & T_{12} \\ T_{21} & T_{22} \end{bmatrix}_{\text{s.c.}} = \frac{1}{1-D^{-2}} \begin{bmatrix} (1+c)-(1-c)D^{-2} & c+cD^{-2} \\ -c-cD^{-2} & (1-c)-(1+c)D^{-2} \end{bmatrix}. \tag{6}$$

By the same token, the chain scattering parameters of a transmission-line section with impedance Z_2, shown in Fig. 3, can be converted to functions in the Z domain as follows:

$$\begin{bmatrix} T_{11} & T_{12} \\ T_{21} & T_{22} \end{bmatrix}_{TLS} = \frac{1}{D^{-1}(1-\Gamma^2)} \begin{bmatrix} 1-\Gamma^2D^{-2} & -(\Gamma-\Gamma D^{-2}) \\ \Gamma-\Gamma D^{-2} & -\Gamma^2+D^{-2} \end{bmatrix} \tag{7}$$

where $\Gamma = (Z_2 - Z_0)/(Z_2 + Z_0)$. The reference planes for both ports are at two connecting points between Z_2 and Z_0.

By cascading open-circuited/short-circuited stubs and transmission-line sections to form a network, the overall chain scattering matrix of the network can be found by the multiplications of the chain scattering matrix of each component, i.e.,

$$\begin{bmatrix} T_{11} & T_{12} \\ T_{21} & T_{22} \end{bmatrix}_{\text{Network}} = \prod_{i=1}^{N} \begin{bmatrix} T_{11}^i & T_{12}^i \\ T_{21}^i & T_{22}^i \end{bmatrix} \tag{8}$$

where N is the number of the components, and T_{11}^i, T_{12}^i, T_{21}^i, and T_{22}^i are the matrix elements representing the ith component.

Assume the network is composed of K open-circuited stubs, L short-circuited stubs, and M transmission-line sections. The fact that the numerators of all the matrix elements in (5)–(7)

have the form of $\alpha_0 + \alpha_1 D^{-2}$ (α_0 and α_1 are real numbers) leads to the following:

$$T_{11}(D) = \frac{\sum_{i=0}^{N} a_i D^{-2i}}{\prod_{k=1}^{K}(1+D^{-2})\prod_{l=1}^{L}(1-D^{-2})\prod_{m=1}^{M}\left(D^{-1}(1-\Gamma_m^2)\right)} \tag{9}$$

where all a_i's are real numbers and can be determined by the characteristic impedances of both stubs and transmission-line sections. In addition, the term $(1+D^{-2})$ comes from each open-circuited stub, the term $(1 - D^{-2})$ comes from each short-circuited stub, and $D^{-1}(1 - \Gamma_m^2)$ comes from the mth transmission-line section.

When the output port of the network uses matched termination, we have $a(2) = 0$ in Fig. 1. The transfer function, denoted as $T(D)$, can then be obtained by the inverse of $T_{11}(D)$, i.e.,

$$\begin{aligned} T(D) &= \left.\frac{b(2)}{a(1)}\right|_{a(2)=0} \\ &= \frac{1}{T_{11}(D)} \\ &= \frac{\prod_{k=1}^{K}(1+D^{-2})\prod_{l=1}^{L}(1-D^{-2})\prod_{m=1}^{M}\left(D^{-1}(1-\Gamma_m^2)\right)}{\sum_{i=0}^{N} a_i D^{-2i}}. \end{aligned} \tag{10}$$

To make (10) in a form proper for the design purpose, we set $z = D^2$, which corresponds a scaling by two on the frequency axis. The transfer function is then modified as follows:

$$T(z) = T(D)|_{z=D^2} = z^{-M/2}\frac{\prod_{k=1}^{K}(1+z^{-1})\prod_{l=1}^{L}(1-z^{-1})}{\sum_{i=0}^{N} A_i z^{-i}} \tag{11}$$

where $A_i = a_i/(\prod_{m=1}^{M}(1 - \Gamma_m^2))$ are functions of the characteristic impedances of both stubs and transmission-line sections. Equation (11) reveals that $T(z)$ has zeros at $z = -1$ (or the normalizing frequency ω_0), which are contributed by the open-circuited stubs, and zeros at dc, which are contributed by the short-circuited stubs. If the zeros contributed from the stubs are removed from $T(z)$, the remaining part of the transfer function is recognized as an AR process multiplied by a term of $z^{-M/2}$ corresponding to some delay. We express the AR process with the function $T_{\mathrm{AR}}(z)$ and we get

$$T_{\mathrm{AR}}(z) = \frac{1}{\sum_{i=0}^{N} A_i z^{-i}}. \tag{12}$$

Since the frequency response of the AR process is uniquely determined by the coefficients A_i and these coefficients are determined by the characteristic impedances of both stubs and transmission-line sections, we could adjust the impedances of these components so that $T_{\mathrm{AR}}(z)$ approximates a proposed AR process.

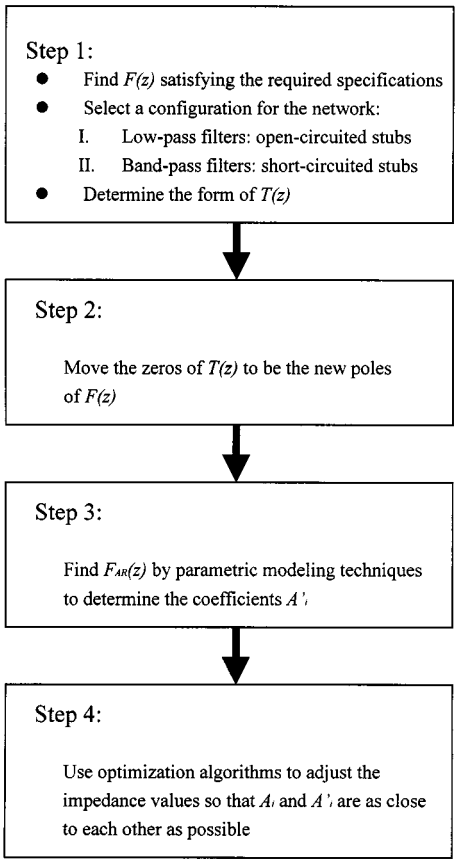

Fig. 4. Design and implementation procedures for the filters.

III. Design and Implementation of Filters

The procedure for design and implementation of filters with transfer functions in the Z domain is illustrated with the aid of the flowchart shown in Fig. 4, and as outlined below.

1) Propose a digital filter prototype $F(z)$, which satisfies the required specifications. Determine the configuration of the network, which attempts to synthesize the function $F(z)$. The configuration can be determined according to the allocations of zeros; e.g., for a low-pass filter prototype, we use open-circuited stubs, and for a bandpass filter prototype, we use short-circuited stubs. The form of transfer function of network $T(z)$ can then be determined by the number of stubs and transmission-line sections used.
2) Divide both $T(z)$ and $F(z)$ by the terms of $T(z)$, which produce zeros at the normalizing frequency, the $(1 + z^{-1})$'s, or at the dc, the $(1 - z^{-1})$'s. We call the function derived from $F(z)$ as $\overline{F}(z)$. In other words, the zeros of $T(z)$ becomes the poles of the function $\overline{F}(z)$.
3) Based on the assumption that the transfer functions of the network, $T(z)$, and the function $F(z)$ are similar to each other, we argue that $T_{\mathrm{AR}}(z)$ and $\overline{F}(z)$ should have similar

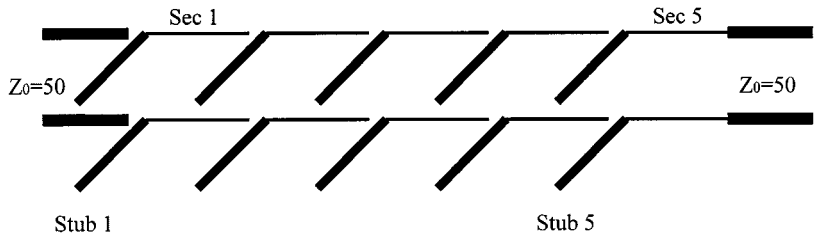

Fig. 5. Configuration of the low-pass filter.

magnitude response in the frequency domain. Since we have known that $T_{\rm AR}(z)$ represents some AR processes, it is reasonable that we try to find an equivalent AR process of the function $\overline{F}(z)$ by parametric modeling techniques. This equivalent AR process is represented by a function $F_{\rm AR}(z)$ as follows:

$$F_{\rm AR}(z) = \frac{1}{\sum_{i=0}^{N} A_i' z^{-i}} \tag{13}$$

where N is the number of the components composing the network.

4) The final step of the whole procedure is to implement the filter. The values of the impedances of the components composing the network are adjusted by using optimization algorithms so that the coefficients of the denominators of $T_{\rm AR}(z)$ and $F_{\rm AR}(z)$ are as close as possible in a specific sense.

This procedure has been used to implement several filters and we find it is featured by the following facets. First of all, the proposed approach takes advantage of the transmission-line sections to improve the filter response; therefore, it is of a nonredundant synthesis method. Furthermore, different from the methods that synthesize filters according to the samples in the frequency domain, this procedure synthesizes filters according to the coefficients representing an AR process. Since the number of the coefficients is usually much less than that of the samples, our approach expedites. This is just as well because an AR process is uniquely defined by one set of coefficients; as long as the coefficient difference between $F_{\rm AR}(z)$ and $T_{\rm AR}(z)$ is small enough, it is guaranteed that the behavior of $F(z)$ follows that of $T(z)$. We have also considered the manufacturing limitation in the design procedure by the designation of the lower and upper bounds of the values of the components. In our experiments, it shows that there exists a tradeoff between the circuit complexity and manufacturing limitation; under a tighter limitation, we can use more components to reach the prescribed performance. This feature shows the adaptability of our approach.

The environment with which we develop our software is MATLAB [13]. The structure of our program is simple, consisting of one main function and another function for optimization. A typical program is composed of about 100 command lines, and its execution time is less than 10 min when a PC with a Pentium-III CPU is used.

In the following, to demonstrate the validity of this proposed approach, we describe the design and implementation of one low-pass filter and one bandpass filter. For both kinds of filters, the reference impedance Z_0 is always equal to 50 Ω.

A. Low-Pass Filters in Microstrip Lines

A low-pass filter with its cutoff frequency equal to 2.0 GHz is first considered. We adopt a prototype $F(z)$ [11] as follows:

$$F(z) = \frac{\sum_{j=0}^{5} b_j z^{-j}}{\sum_{i=0}^{5} a_i z^{-i}} \tag{14}$$

where $\{b_j, 0 \le j \le 5\} = \{0.0528,, 0.2639, 0.5279, 0.5279, 0.2639, 0.0528\}$, and $\{a_i, 0 \le i \le 5\} = \{1.0000, 0.0000, 0.6334, 0.0000, 0.0557, 0.0000\}$. This prototype is a Butterworth low-pass filter with its cutoff frequency equal to $0.5\,\omega_0$. In other words, the normalizing angular frequency ω_0 is now $2\pi \times (4 \times 10^9)$ rad/s. There are exactly five zeros at the normalizing frequency, or at $z = -1$, which are to be canceled by the zeros of transfer function of the network when we are trying to find the function $\overline{F}(z)$. This low-pass filter is implemented with a network of the configuration shown in Fig. 5. Since there are five open-circuited stubs and five transmission-line sections interlaced, the transfer functions of the network also has five zeros at the normalizing frequency. As a result, the coefficients A_i' associated with the $F_{\rm AR}(z)$ can be found directly by the denominator of $F(z)$. That is, $A_i' = a_i/b_0$ for $0 \le i \le 5$ and $A_i' = 0.0$ for $6 \le i \le 11$.

With the function for optimization, the values of the characteristic impedances of both the stubs and transmission-line sections are adjusted according to the goal that the difference between A_i's and A_i''s is minimized in the sense of least-mean-square (LMS) error. In other words, we want to minimize the value of $\sum_{i=0}^{11}(A_i - A_i')^2$. Furthermore, due to the limitation caused by fabrication techniques, the values of the characteristic impedances of all components are limited to be between 15–150 Ω. The optimization algorithms give the characteristic impedance values (in ohms) of both stubs and transmission-line sections to be (150-49.9)–(35.7-99.4)–(23.3-92.7)–(34.0-65.5)–(150-41.8); in each parenthesis, the first value represents an open-circuited stub and the second value represents a transmission-line section.

The magnitude response of the transfer function of the filter $|T(z)|$ and that of the proposed idea filter $|F(z)|$ are both shown in Fig. 6, in which the cutoff frequency has been scaled to be 2.0 GHz. Note that, except for small ripples occurring in $|T(z)|$

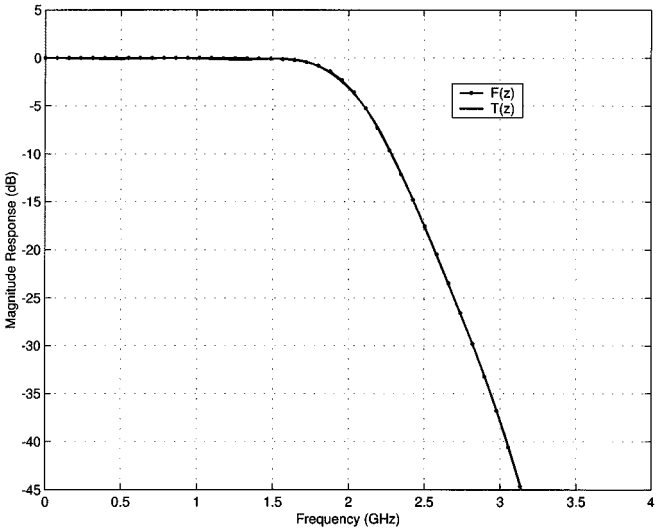

Fig. 6. Magnitude responses of $F(z)$ and $T(z)$ for the low-pass filter with a cutoff frequency at 2.0 GHz.

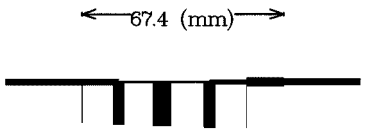

Fig. 7. Layout of the low-pass filter in the form of a microstrip line.

over the passband frequencies, $|T(z)|$ inherits the most important characteristics of $|F(z)|$: the location of the 3-dB corner and attenuation slope beyond the cutoff frequency. This implies that using A_i' as the target and using LMS error as the constraint are proper strategies for the optimization algorithms to implement the low-pass filter.

The filter is fabricated in the form of microstrip lines. The substrate used is Duroid, of which the relative dielectric constant is 2.5 and the height is 0.787 mm (31 mil). The layout of the filter is shown in Fig. 7. The left-hand side is port 1, and the right-hand side is port 2. On both sides, the reference impedance lines (50 Ω) are placed. All components have the ideal electrical length 90° at 4.0 GHz; however, to account for the effects of discontinuities, the physical lengths of the components have been modified. The total length of the filter is 67.4 mm. We measure the reflected and transferred parameters by using an HP 8510C network analyzer. The result is presented in Fig. 8. Although the 3-dB corner moves to around 1.96 GHz because of both the conductor and dielectric losses, the result proves the effectiveness of our design/implementation approach.

B. Bandpass Filters in Microstrip Lines

We address design and implementation of a bandpass filter in this section. The central frequency of the filter is 3 GHz; therefore, the normalizing angular frequency ω_0 is equal to $2\pi \times (3 \times 10^9)$ rad/s. The bandwidth is set to be 40%. We cascade the basic circuit shown in Fig. 9 to form a bandpass filter. Since each basic circuit has two short-circuited stubs, it contributes two zeros at dc. Note that because the transfer function of the network is a periodic function with the period being $2\omega_0$, each basic circuit also contributes two zeros at $2\omega_0$.

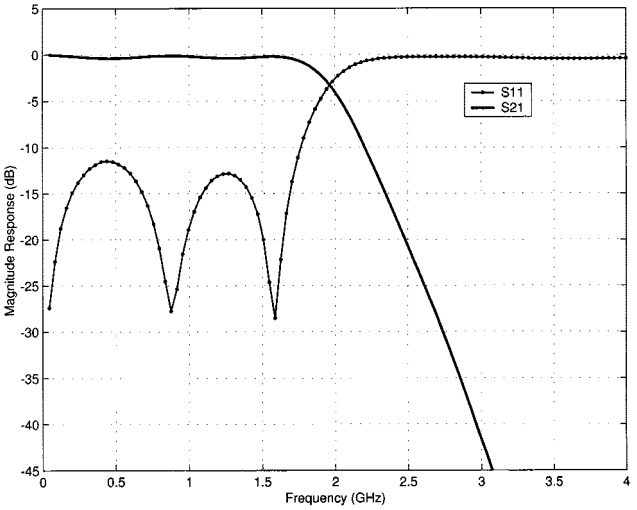

Fig. 8. Reflected and transferred scattering coefficients at port 1 of the low-pass filter.

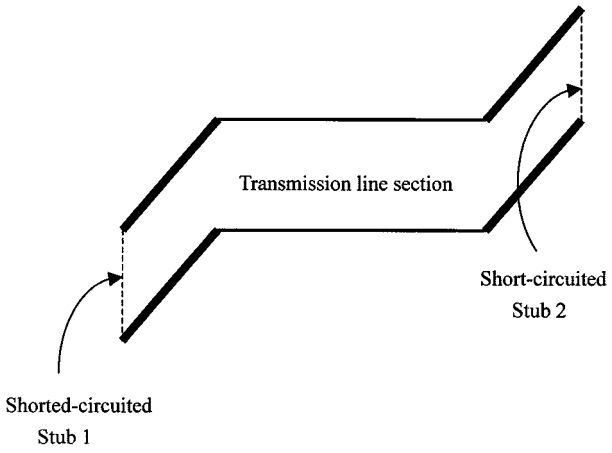

Fig. 9. Configuration of the basic circuit to compose bandpass filters.

For the bandpass filter, the prototype is given as follows:

$$F(z) = \frac{\sum_{j=0}^{4} b_j z^{-j}}{\sum_{i=0}^{4} a_i z^{-i}} \tag{15}$$

where $\{b_j, 0 \le j \le 4\} = \{0.0048, -0.0193, 0.0289, -0.0193, 0.0048\}$ and $\{a_i, 0 \le i \le 4\} = \{1.0000, 2.3695, 2.3140, 1.0547, 0.1874\}$. Since we use seven basic circuits to implement this filter, the prototype is divided by $(1 - z^{-1})^{14}$ to obtain the corresponding $\overline{F}(z)$. $\overline{F}(z)$ is then transformed to an equivalent AR process. By the same optimization algorithm, which minimizes the difference between A_i of $T_{\mathrm{AR}}(z)$ and A_i' of $F_{\mathrm{AR}}(z)$ in the sense of LMS error, we obtain the characteristic impedances values (in ohms) of both short-circuited stubs and transmission-line sections, which are (27.1-98.6-49.5)–(98.9-96.3-89.5)–(93.3-64.2-108.1)–(47.5-53.7-92.0)–(56.3-77.1-64.8)–(75.8-94.0-31.7)-(85.9-59.9-27.3). In each parenthesis, the first two numbers are the characteristic impedances of the stubs and the last

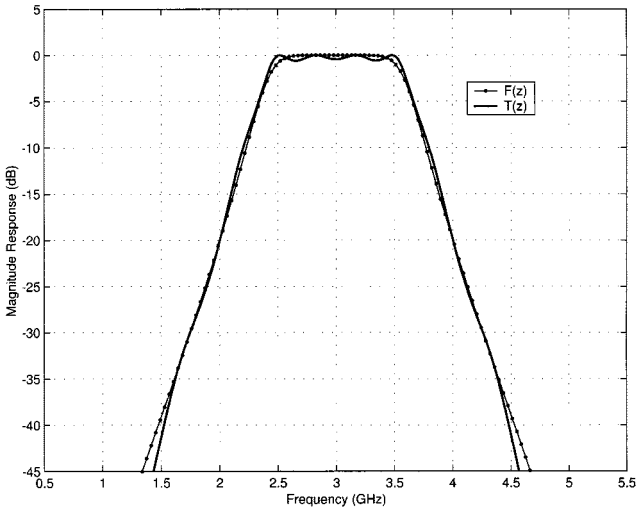

Fig. 10. Magnitude responses of $F(z)$ and $T(z)$ for the bandpass filter with central frequency at 3.0 GHz and bandwidth of 40%.

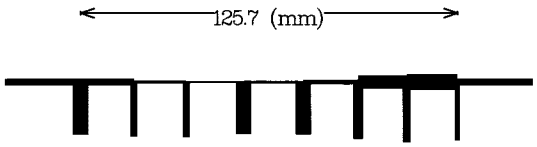

Fig. 11. Layout of the bandpass filter with bandwidth of 40% in the form of microstrip line. Note that each shunt stub is wrapped around to the ground.

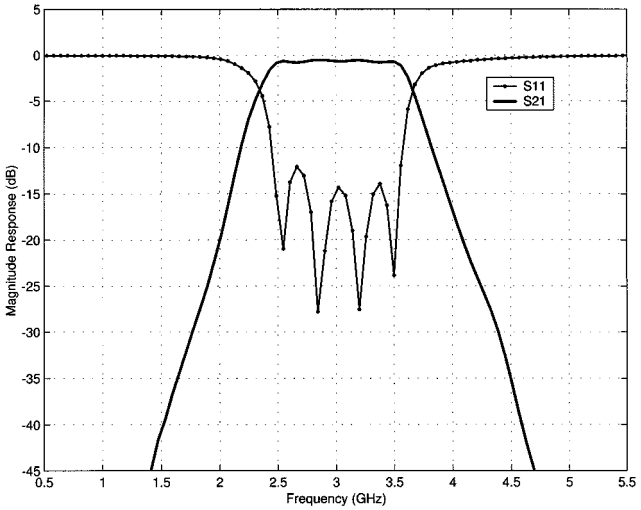

Fig. 12. Reflected and transferred scattering coefficients at input and output ports for the bandpass filter shown in Fig. 11.

one is the characteristic impedance of the transmission-line section. Since the second stub of each parenthesis (except the last parenthesis) and the first stub of the next parenthesis are parallelly connected, we can use a single stub with their equivalent characteristic impedance to replace the double stubs.

The magnitude responses of both $F(z)$ and $T(z)$ are shown in Fig. 10. The ripples of $|T(z)|$ over the passband frequencies are around 0.5 dB. The insertion loss rate of $|T(z)|$ is in good agreement with that of $|F(z)|$ for the frequencies outside the passband. The strategy using A_i' as the target and LMS error as the constraint for the optimization consideration satisfies the need for the design of bandpass filters.

This bandpass filter is also implemented on the Duroid substrate mentioned previously, and its layout is shown in Fig. 11. The frequency responses of the filter are measured and shown in Fig. 12, where the ripple over the passband is less than 0.3 dB. Moreover, the insertion loss rate of the filter response outside the passband is in good agreement with that of the postulated value.

The experimental results for several bandpass filters with different bandwidth requirements show that: 1) it is easier to find appropriate solutions (the values of characteristic impedance) for filters that have wider bandwidth and 2) with the same attenuation rate outside the passband, more basic circuits are required to implement filters that have narrower bandwidth.

IV. Conclusion

A new approach to design and implement low-pass and bandpass microwave filters has been proposed in this paper. Combining the design and implementation phases in a framework, this approach is featured by the utilization of well-developed DSP techniques and optimization algorithms, which makes it suitable for computer-aided design (CAD) applications. In addition, including the consideration of characteristic impedances of transmission-line sections during the implementation phase, this approach provides different configurations for filters other than those conventional structures that are based on lumped-element consideration and Richard's transformation. Both low-pass and bandpass filters are fabricated in microstrip lines to validate this new approach at microwave frequencies. The experimental results conclude the usefulness of this new approach.

References

[1] G. L. Matthaei, L. Young, and E. M. T. Jones, *Microwave Filters, Impedance-Matching Networks, and Coupling Structures*. Norwood, MA: Artech House, 1980.

[2] P. P. Roberts and G. E. Town, "Design of microwave filters by inverse scattering," *IEEE Trans. Microwave Theory Tech.*, vol. 43, pp. 739–743, Apr. 1995.

[3] M. L. Roy, A. Pérennec, S. Toutain, and L. C. Calvez, "The continuously varying transmission-line technique—Application to filter design," *IEEE Trans. Microwave Theory Tech.*, vol. 47, pp. 1680–1687, Sept. 1999.

[4] S. B. Cohn, "Parallel-coupled transmission-line-resonator filters," *IRE Trans. Microwave Theory Tech.*, vol. MTT-6, pp. 223–231, Apr. 1958.

[5] M. Tran and C. Nguyen, "Modified broadside-coupled microstrip lines suitable for MIC and MMIC applications and a new class of broadside-coupled bandpass filters," *IEEE Trans. Microwave Theory Tech.*, vol. 41, pp. 1336–1342, Aug. 1993.

[6] P. I. Richard, "Resistor-transmission line circuits," *Proc. IRE*, vol. 36, pp. 217–220, Feb. 1948.

[7] K. Kuroda, "General properties and synthesis of transmission-line networks," in *Microwave Filters and Circuits*, A. Matsumoto, Ed. New York: Academic, 1970, vol. 22.

[8] D. M. Pozar, *Microwave Engineering*, 2nd ed. New York: Wiley, 1998.

[9] T.-W. Pan and C.-W. Hsue, "Modified transmission and reflection coefficients of nonuniform transmission lines and their applications," *IEEE Trans. Microwave Theory Tech.*, vol. 46, pp. 2092–2097, Dec. 1998.

[10] R. Tascone, P. Savi, D. Trinchero, and R. Orta, "Scattering matrix approach for the design of microwave filters," *IEEE Trans. Microwave Theory Tech.*, vol. 48, pp. 423–430, Mar. 2000.

[11] A. V. Oppenheim and R. W. Schafer, *Discrete-Time Signal Processing*. Englewood Cliffs, NJ: Prentice-Hall., 1989.

[12] S. Haykin, *Adaptive Filter Theory*. Englewood Cliffs, NJ: Prentice-Hall, 1996.

[13] D. Hanselman and B. Littlefield, *Mastering MATLAB 5*. Englewood Cliffs, NJ: Prentice-Hall, 1998.

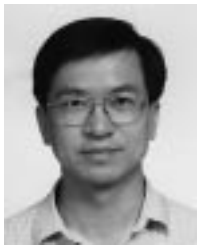

Da-Chiang Chang was born in Taipei, Taiwan, R.O.C., in 1966. He received the B.S. and M.S. degrees in electrical engineering from the National Tsing-Hua University, Hsin-Chu, Taiwan, R.O.C., in 1989 and 1991, respectively, and is currently working toward the Ph.D. degree in electronic engineering at the National Taiwan University of Science and Technology, Taipei, Taiwan, R.O.C.

From July 1991 to June 1993, he served as an Officer in the R.O.C. Air Force. In Fall 1993, he joined the Department of Electronic Engineering, Chinese Institute of Technology, where he is currently an Instructor. His current interests are in discrete-time signal processing, wireless communications, and RF and analog circuit design.

Ching-Wen Hsue (SM'91) was born in Tainan, Taiwan, R.O.C. He received the B.S. and M.S. degrees in electrophysics and electronic from the National Chiao-Tung University, Hsin-Chu, Taiwan, R.O.C., in 1973 and 1975, respectively, and the Ph.D. degree from the Polytechnic University (formerly the Polytechnic Institute of Brooklyn), Brooklyn, NY, in 1985.

From 1975 to 1980, he was a Research Engineer in the Telecommunication Laboratories, Ministry of Communication, Taiwan, R.O.C. From 1985 to 1993, he was a Member of Technical Staff with Bell Laboratories, Princeton, NJ. In 1993, he joined the Department of Electronic Engineering, National Taiwan University of Science and Technology, Taipei, Taiwan, R.O.C., as a Professor, where, from August 1997 to July 1999, he served as the Department Chairman. His current interests are in pulse-signal propagation in lossless and lossy transmission media, wave interactions between nonlinear elements and transmission lines, photonics, high-power amplifiers, and electromagnetic inverse scattering.